Sensitivity study of ice crystal optical properties in the 874 GHz submillimeter band

Guanglin Tang[1], Ping Yang[1], Dong L. Wu[2]

1. Department of Atmospheric Sciences, Texas A&M University, College Station, TX

2. Climate and Radiation Lab, NASA Goddard Space Flight Center, Greenbelt, MD

For publication in the
Journal of Quantitative Spectroscopy and Radiative Transfer

Corresponding author address: Prof. Ping Yang, Department of Atmospheric Sciences, Texas A&M University, College Station, TX 77845. Email: pyang@tamu.edu

Abstract

Testing of an 874 GHz submillimeter radiometer on meteorological satellites is being planned to improve ice water content retrievals. In this paper we study the optical properties of ice cloud particles in the 874 GHz band. The results show that the bulk scattering and absorption coefficients of an ensemble of ice cloud particles are sensitive to the particle shape and effective diameter, whereas the latter is also sensitive to temperature. The co-polar back scattering cross-section is not sensitive to particle shape, temperature, and the effective diameter in the range of 50-200μm,.

Keywords: Ice crystals, Optical properties, 874 GHz, Submillimeter

Introduction

One of the largest uncertainties in understanding the current climate and possible future changes is the radiative forcing of ice clouds [1]. The main difficulty in quantifying the radiative characteristics of ice clouds is that many factors (or the degrees of freedom, DOF) affect the radiative forcing, such as ice water content (IWC), ice particle size distribution (PSD), individual particle shape, temperature and cloud height [2]. Almost all applications such as climate models parameterize some of these factors to decrease DOF in order to simplify calculations [3]. For example, in radiative transfer models (RTMs), the PSD is often assumed as a gamma distribution with respect to particle maximum dimension (D_m) with a certain shape parameter and a scale parameter. An ensemble of the individual particles are assumed to be a certain mixture of various habits in some advanced RTMs. Other common simplifications are to assume that the temperature and IWC are vertically uniform, or the cloud height is assumed to be fixed at a certain level. The validation of these parameterizations is a challenging task from both observational and theoretical perspectives.

Currently, ice clouds are observed using multiple tools including in situ instruments and remote sensors such as ground-based radars, lidars, and radiometers, and airborne, balloon-borne, and satellite-based instruments. In situ instruments such as airborne particle samplers provide the most precise measurement but suffer from very limited time and spatial coverage. Radars, lidars, and radiometers are used to retrieve ice cloud properties from their received radiances, but all the aforementioned factors that affect radiative forcing must be considered. Most retrieval methods utilize RTMs as their cores so it is desirable to develop the best parameterizations of all factors that match between the RTM simulated and instrument observed radiances throughout several spectral bands [3] [4]. The ideal condition to retrieve a particular quantity (e.g., IWC) is when the radiance is only sensitive to the target quantity while not sensitive to any other quantity (such as temperature, or particle shape, etc). Ground-based instruments have more spatial and time coverage than in situ measurement and are more economic and easily handled than satellites. However, the retrievals of high altitude ice clouds from ground-based instruments are interfered with significantly by aerosols and absorbing gases in the lower troposphere. Current radiometers on satellites receive radiance covering visible, near and far (thermal) infrared, and millimeter bands [5]. When ice cloud is present, visible and infrared radiances observed by satellite sensors are usually sensitive to ice particle shape, while millimeter and submillimeter radiances measured by spaceborne instruments and radars are sensitive to particle size distributions. Specially, two submillimeter bands, 642GHz (including horizontal and vertical polarization states, H&V) and 874GHz, provided by the Compact Scanning Submillimeter-wave Imaging Radiometer (CoSSIR, flying on an airplane at about 20km height), have been successfully used to retrieve IWC [4]. Additionally, infrared bands on satellites can only "see" very high ice clouds (i.e., over 7-8km), while visible and millimeter band signals are contaminated by radiation from lower liquid clouds, water vapor, and the surface. Submillimeter bands can not only see through ice clouds with moderate transmission and absorption, but also exclude interference from lower liquid clouds, water vapor, and the surface due to high absorption by water vapor. Considering these features of submillimeter wavelengths, to better observe global IWC, NASA supports installing submillimeter radiometers on satellites. One of such instruments is an 874GHz submillimeter receiver onboard a satellite platform with a lower earth orbit. Thus, it is necessary to study the ice cloud optical properties in this band to fully understand the information content of this channel for remote sensing of ice cloud properties.

A retrieval of ice cloud properties from a satellite or radar instrument requires a lookup table listing appropriate optical properties with respect to a certain set of assumed parameterizations of input properties, such as PSD, IWC, particle shape, temperature, and cloud height. The largest uncertainty of the parameterization lies in ice particle shape. Natural ice particles exhibit a very large range of geometries, from simple pristine prisms to complex irregular aggregates. In addition, ice particle surfaces can be smooth or rough to various degrees. They can also be attached to, e.g., soot particles, or include aerosols and air bubbles. All of these factors affect the optical properties of ice particles, especially when wavelengths are comparable to or larger than particle sizes. A good parameterization of ice particle shapes leads to good agreements between observations and simulations, and allows a simplified parameterization of other factors such as IWC and PSD. In the Moderate Resolution Imaging Spectroradiometer (MODIS) collection 6 (C6), a simple single compact hexagonal-column-ice-crystal-aggregate habit with severer roughness was used instead of an 11-habit mixture for the MODIS collection 5 (C5) model [6] [7]. Similarly, Liu et al [8] proposes a two-habit model (THM) to reduce inconsistent retrieval results among spectral bands. In addition, many other particle shapes have been considered [9] [10] [11] [12] [13].

In this paper, we focus on studying the sensitivity of ice cloud optical properties to various factors, including particle shape, PSD and temperature, in the 874GHz band. The optical properties of individual ice particles are be computed using a state-of-the-art invariant imbedding T-matrix method (IITM) developed at Texas A&M University [14] [15]. Note, various numerous techniques have been developed for the simulation of the single-scattering properties of ice crystals [16-18]. In this study, ice particles are assumed to be randomly oriented. Because most high-cloud ice particles are smaller than or comparable to the considered wavelength (343μm), the effect of surface roughness is insignificant. Therefore, all particles are assumed to be smooth in this paper.

1. Refractive index of ice

To the best of the authors' knowledge, direct measurement of the refractive index of ice near 874GHz was reported only by Zhang et al. [19] with errors of ±0.002 for the real part and ±0.0005 for the imaginary part using time domain spectroscopy. However, their measurement covers a relatively small range of temperature, 239-263K. We cover 160-270K following the procedure described by Iwabuchi and Yang [20]. Specfically, we compute the imaginary part of the refractive index in the wavelength range of 0.3μm-2m using several datasets [21-27], and, then, perform the iterative Kramers-Kronig (KK) analysis [20,28] to obtain the real part of the refractive index and the absorption strength in the wavelength range 0-0.3μm and 2m-∞. During the iteration, the computed real part of the refractive index is compared with the observed values at 0.5893μm, 0.632μm, and

1m to determine the status of convergence. Our procedure is also consistent with the procedure used in the new completion by Warren and Brandt [21]. Particularly, in the wavelength range of 300μm-2m, the imaginary part is computed using the theoretical formula with empirical coefficients described by Matzler [22]. During this process, the temperature dependence is considered, which is assumed to be an exponential dependence of the imaginary part of the refractive index on the temperature. We perform this process for temperature between 160K-270K with an increment of 10K . Figure 1 shows the variations of the real and imaginary parts of the refractive index at 874 GHz with respect to temperature. The differences between the present compilation and the Zhang et al. measurements are less than 0.1% for the real part and 2% for the imaginary part, which is less than or near to the errors of measurement. The variation of the real part with respect to temperature is weak, only around 1% difference between 160K and 270K, indicating weak sensitivity of the scattering coefficient and phase matrix to temperature. Unlike visible bands, the imaginary part (absorption) at the 874GHz is non-negligible and significantly sensitive to temperature, with a factor of 3 increase between 160K and 270K.

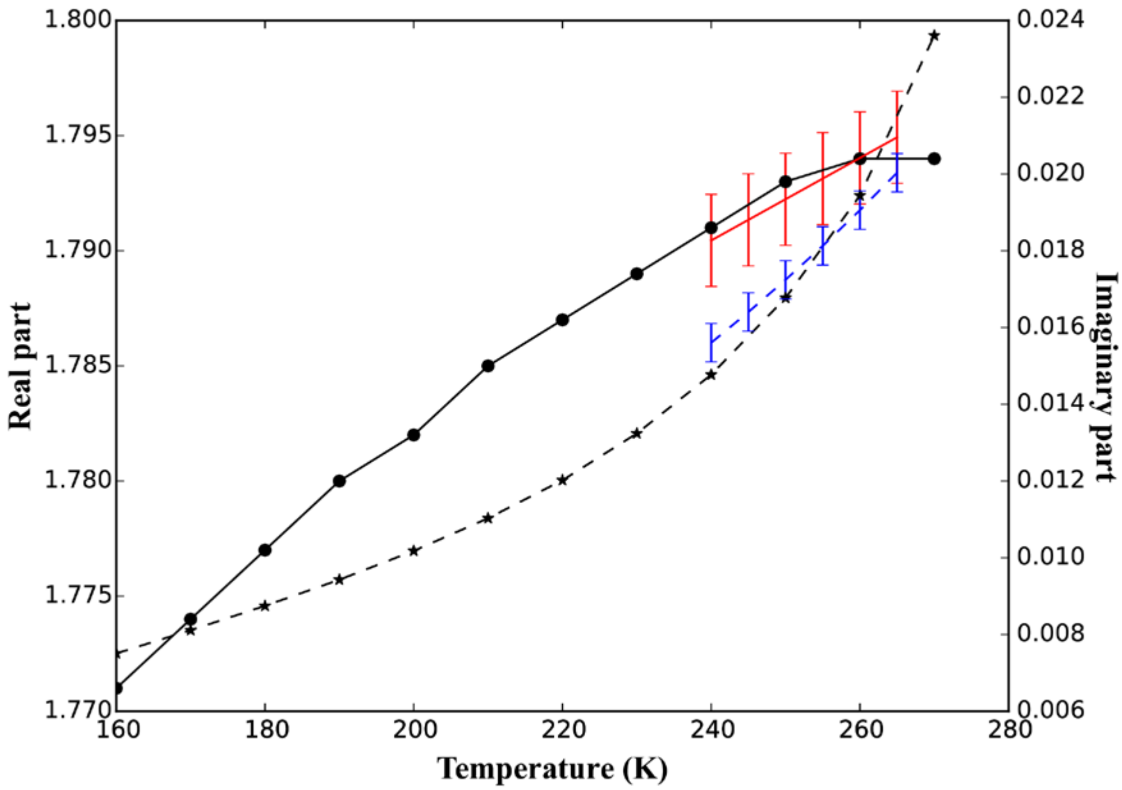

Figure 1. The real (solid black line) and imaginary (dashed black line) parts of ice refractive index as a function of temperature in our compilation. The measured real (red solid line) and imaginary (blue dashed line) parts are also plotted, along with error bars.

2. Sensitivity to shape and size: Two habit model versus MODIS C6

Two parameterizations of ice particle shapes, THM and MODIS C6, are compared to study the sensitivity of ice particle optical properties to shapes. The PSD is parameterized as a gamma distribution with respect to particle maximum dimension (D_m, defined as the side length for hexagonal columns or the maximum distance between two points for aggregates) with a dimensionless dispersion of 0.1 in the form

$$n(D_m) = N_0 D_m^{0.1} e^{-\lambda D_m}, \quad (1)$$

where $n(D_m)$ represents number of ice particles per unit mass of bulk ice particles per size bin at D_m, in a unit of $g^{-1}\mu m^{-1}$, N_0 is the intercept, and λ is the slope. The two constants N_0 and λ are dependent according to conservation of mass:

$$\int_0^{\infty} n(D_m)m(D_m)dD_m = 1, \quad (2)$$

where $m(D_m)$ represents the mass of an individual ice particle with size D_m. Therefore, given a certain ice particle shape parameterization, the DOF of the PSD is 1. Hence, the PSD can be represented by a single variable, the median mass diameter, D_{mm}, meaning that half of total mass is smaller than D_{mm}:

$$\int_0^{D_{mm}} n(D_m)m(D_m)dD_m = \frac{1}{2}. \quad (3)$$

It can be proved that D_{mm} and $n(D_m)$ are mappable into each other for a given $m(D_m)$. A more commonly used parameterization for PSD is the so-called effective size, which is defined by:

$$D_{eff} = 1.5\frac{\int_0^{\infty} n(D_m)V(D_m)dD_m}{\int_0^{\infty} n(D_m)A(D_m)dD_m}, \quad (4)$$

where D_{eff} indicates the effective size for a given PSD, $V(D_m)$ and $A(D_m)$ the volume and average projected area of individual particles.

Figure 2 shows the variation of scattering coefficient (unit is m^2g^{-1}) versus D_{eff} for both THM and MODIS C6 at 240K. The calculation of single scattering properties is performed for D_m in a range of 10-1000 μm with an increment of 10 μm. At around tens to hundreds of microns, which are typical sizes of ice cloud particles, the scattering coefficient is sensitive to PSDs for either habit. Also note that the scattering coefficient is sensitive to particle shape when particle sizes are comparable to or larger than the wavelength (343μm). Figure 3 is the same as Figure 2 but for the variation of absorption coefficient. Similar sensitivities to PSD and particle shape are observed. Also note that little of the attenuated energy is absorbed when D_{eff} is small, while about 5-10% is absorbed when D_{eff} is larger than about 50μm. These sensitivities increase uncertainties in IWC retrievals.

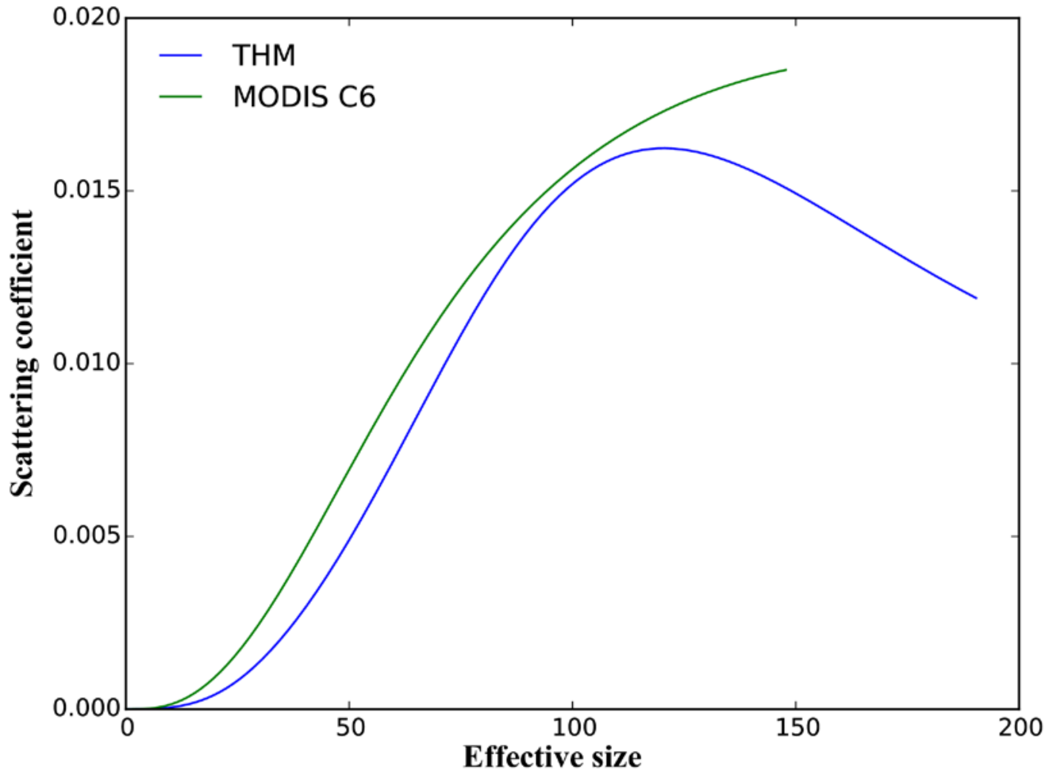

Figure 2. The scattering coefficients (m^2g^{-1}) of THM and MODIS C6 ice particle shape habits as functions of effective size (μm) at 240K.

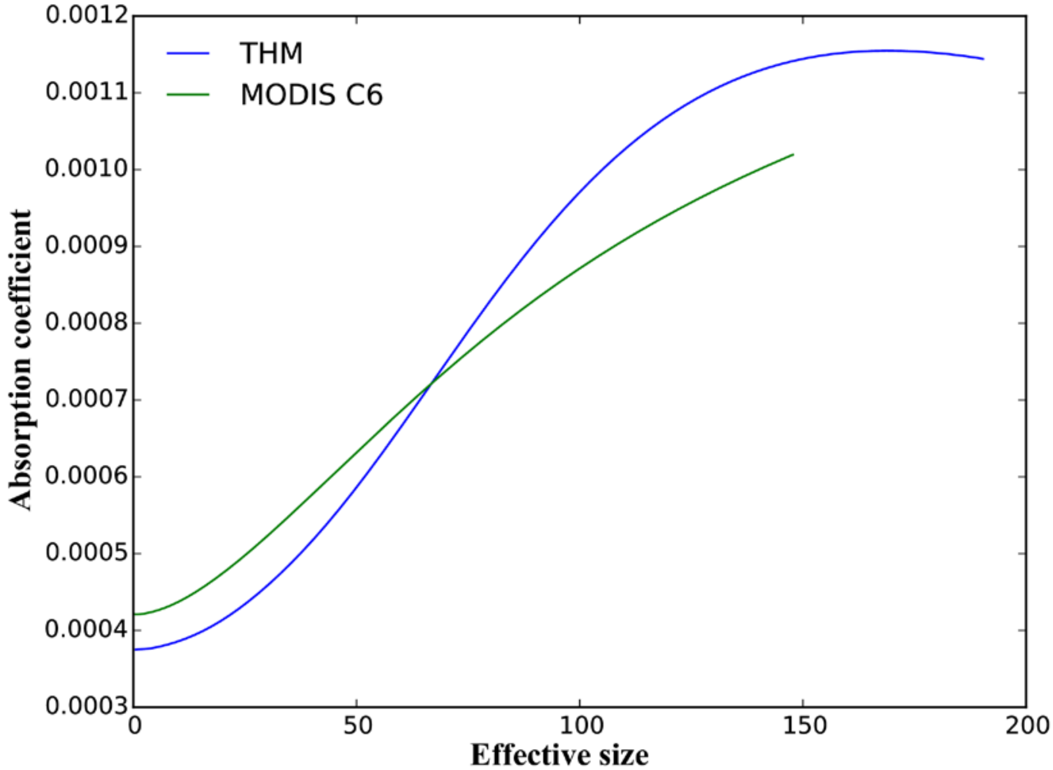

Figure 3. The same as Fig. 2 but showing the absorption coefficients.

To test the sensitivity of the radiances observed by satellite sensors to the particle shape and size in the realistic atmospheres, we perform RTM simulations using the Discrete Ordinates Radiative Transfer Model (DISORT) [29]. In the simulations an ice cloud is assumed to locate between 10-12km, with a uniform temperature of 230K. The atmospheric vertical profile is the US standard atmosphere for the tropics. Figure 4 shows the variation of nadir view brightness temperature at TOA with D_{eff}. As expected, larger IWP leads to a lower brightness temperature at TOA. When D_{eff} is around 50µm, The THM and MODIS C6 give similar brightness temperatures. However, when D_{eff} is around 100µm, the brightness temperatures for THM are about 10K lower than the counterparts of the MODIS C6. When D_{eff} is small, the optical thickness of the cloud is also small, which corresponds to a near clear sky case. In this case, the brightness temperature is about 254K, which is bellow the freezing point, resulting from sufficient absorption by water vapor in the lower atmosphere. The information content bellow 5km cannot be seen from the TOA in the 874GHz band. Thus, the nadir view brightness temperature at TOA is sensitive to the particle size and the particle shape when D_{eff} is around 100μm, which is a common value for real clouds. Additionally, the brightness temperature is sensitive to IWP.

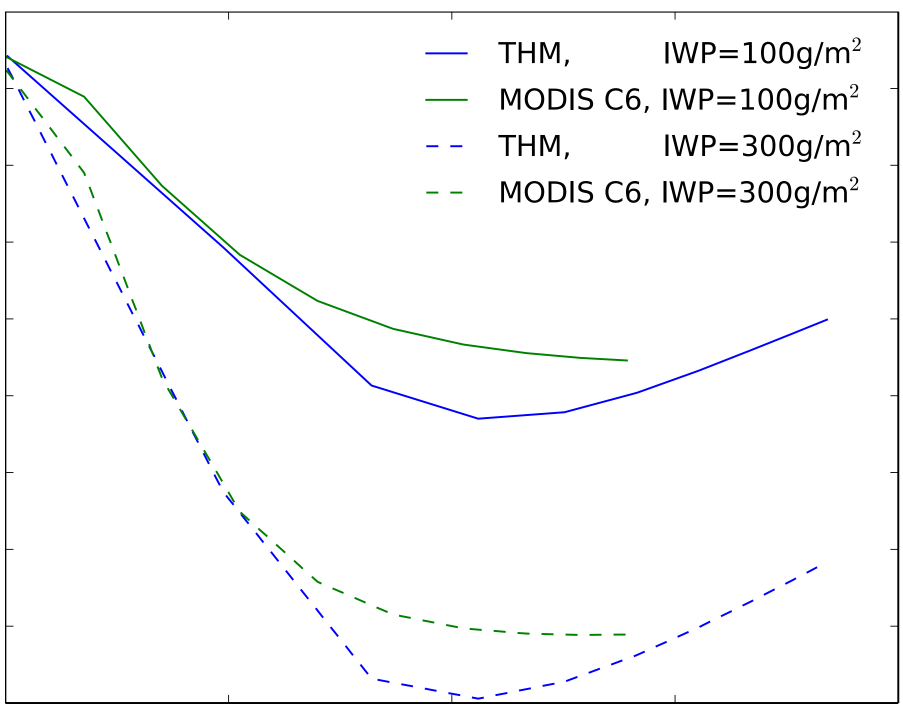

Figure 4. The nadir view brightness temperature at TOA as a function of the effective size.

3. Sensitivity to temperature

Figures 5 and 6 show the scattering and absorption coefficients as functions of both D_{eff} and temperature. It is evident that the scattering coefficient is insensitive, while the absorption coefficient is sensitive to temperature. This is a good feature that can help to retrieve the vertical profile of IWC from satellites. But this requires a priori knowledge of the vertical temperature profile, without which the IWC retrieval can be even worse instead.

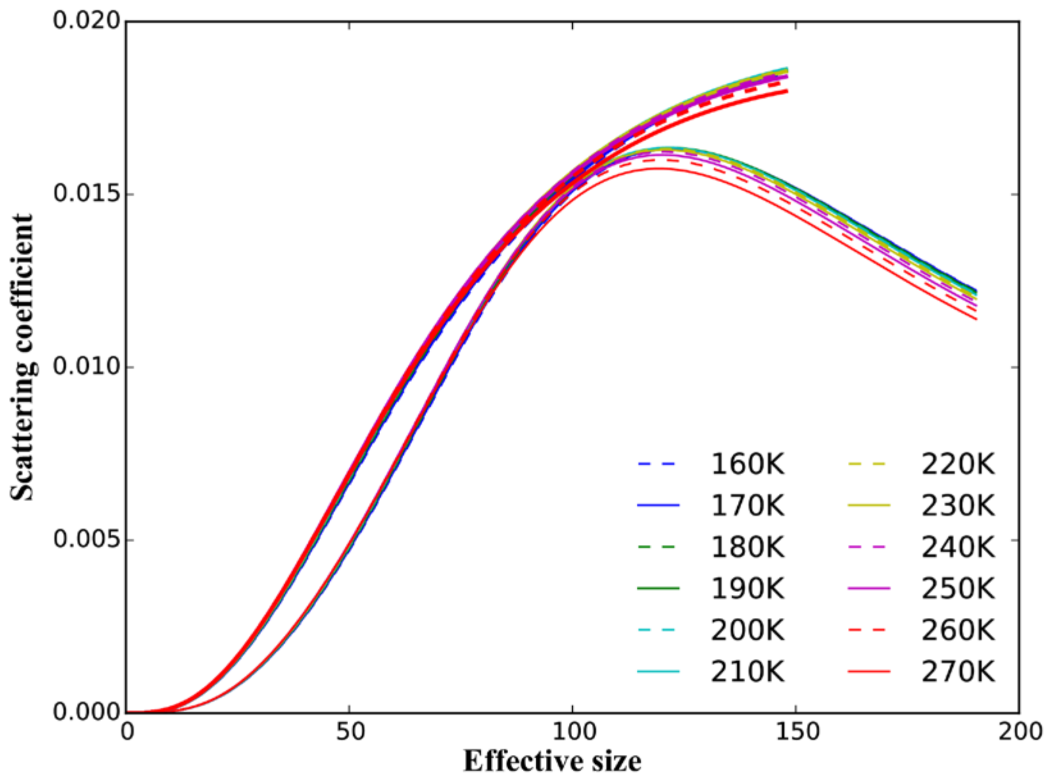

Figure 5. The scattering coefficient as a function of D_{eff} for various temperatures. Thin (thick) lines indicate THM (MODIS C6) habit.

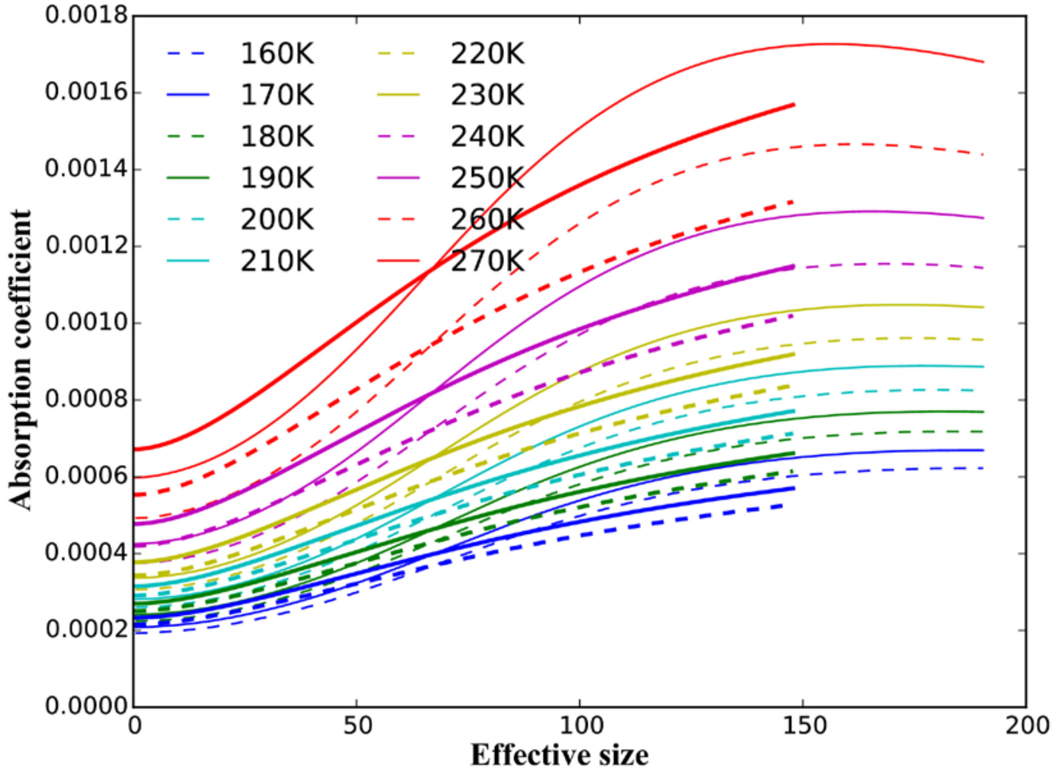

Figure 6. The same as Fig. 5 but showing the absorption coefficient.

In the previous RTM simulations, the cloud temperature is 230K, which is the same as the ambient. To test the sensitivity of the TOA brightness temperature to the refractive index, we keep the cloud temperature of 230K, but use the single optical properties at a different temperature, e.g., 270K. The result is shown in Figure 7. Evidently, the brightness temperature is sensitive to the temperature at which the single optical properties are computed. The difference between 230K and 270K is greater than 5K when D_{eff} is larger than 50µm and greater than 10K when D_{eff} is larger than 70µm. This suggests that neglecting the temperature dependence of the single-scattering properties can lead to large bias of simulated brightness temperature. Thus, to retrieve vertical profile of IWC, this temperature dependence must be considered.

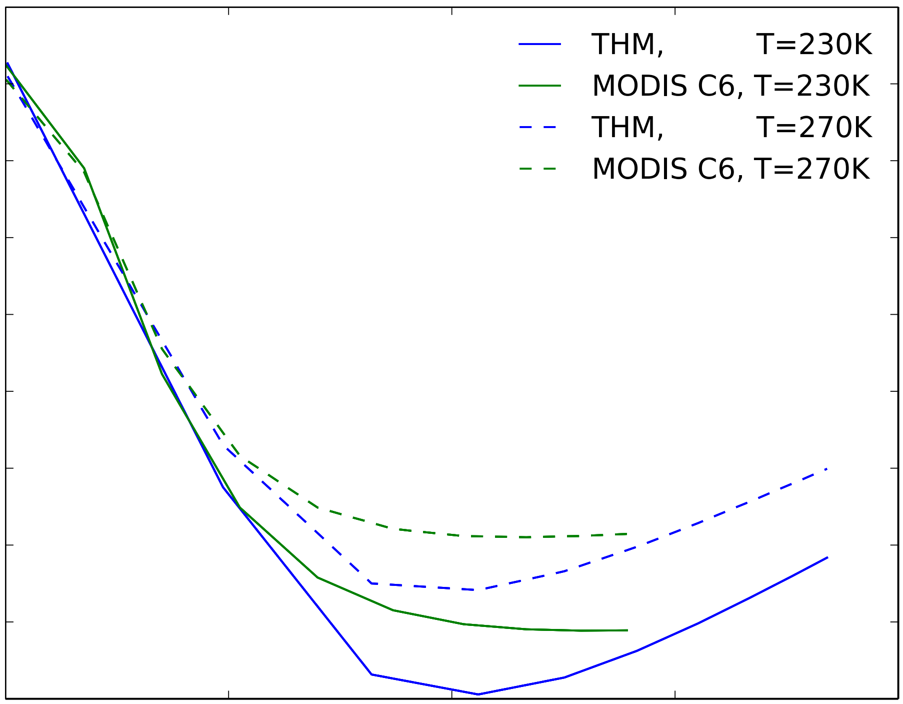

Figure 7. The nadir-view brightness temperature at TOA as a function of the effective size. The IWP is 300g/m^2. Solid lines are the original RTM simulation. Dashed lines are the RTM simulations where cloud single optical properties at 270K are used.

Figure 8 shows the horizontal-horizontal polarization (h-h, transmitting and receiving both horizontal) back scattering cross-section (σ_{hh}) in units of db, where db is defined as $1\text{db} = 10 \times \log_{10}(1\text{g/m}^2)$. The vertical-vertical (v-v, transmitting and receiving both vertical) cross-section (σ_{vv}) is the same as σ_{hh} due to the random orientation of particles. Figure 9 shows the horizontal-vertical polarization (h-v, transmitting horizontal and receiving vertical) back scattering cross-section (σ_{hv}). The vertical-horizontal polarization (v-h, transmitting vertical and receiving horizontal) back scattering cross-section (σ_{vh}) is the same as σ_{hv} due to the random orientation condition. Clearly, neither of σ_{hh} and σ_{hv} is sensitive to temperature, which is consistent with the insensitivity of the real part of the refractive index to temperature. σ_{hh} is relatively less sensitive to particle shape and D_{eff} when D_{eff} is larger than about 50μm, while σ_{hv} is relatively more sensitive to both particle shape and D_{eff}. This insensitivity of σ_{hh} and σ_{vv} to particle shape, temperature and D_{eff} can enhance the accuracy of retrieving IWCs from meteorological radars, which measure σ_{hh} or both σ_{hh} and σ_{vv}. However, a ground based radar in the 874GHz may not be useful to retrieve IWCs, because the transmitted signal is fully absorbed by lower atmospheric water vapor.

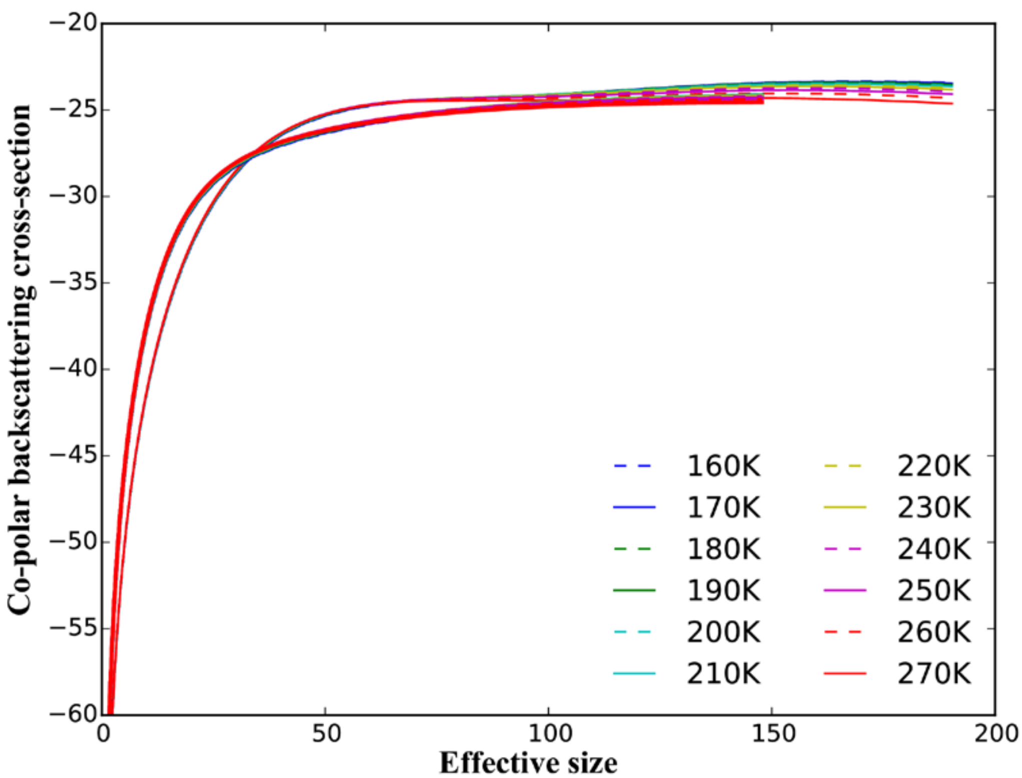

Figure 8. The back scattering cross-section (db) for polarization h-h as a function of D_{eff} and temperature. Thin (thick) lines indicate THM (MODIS C6) habit.

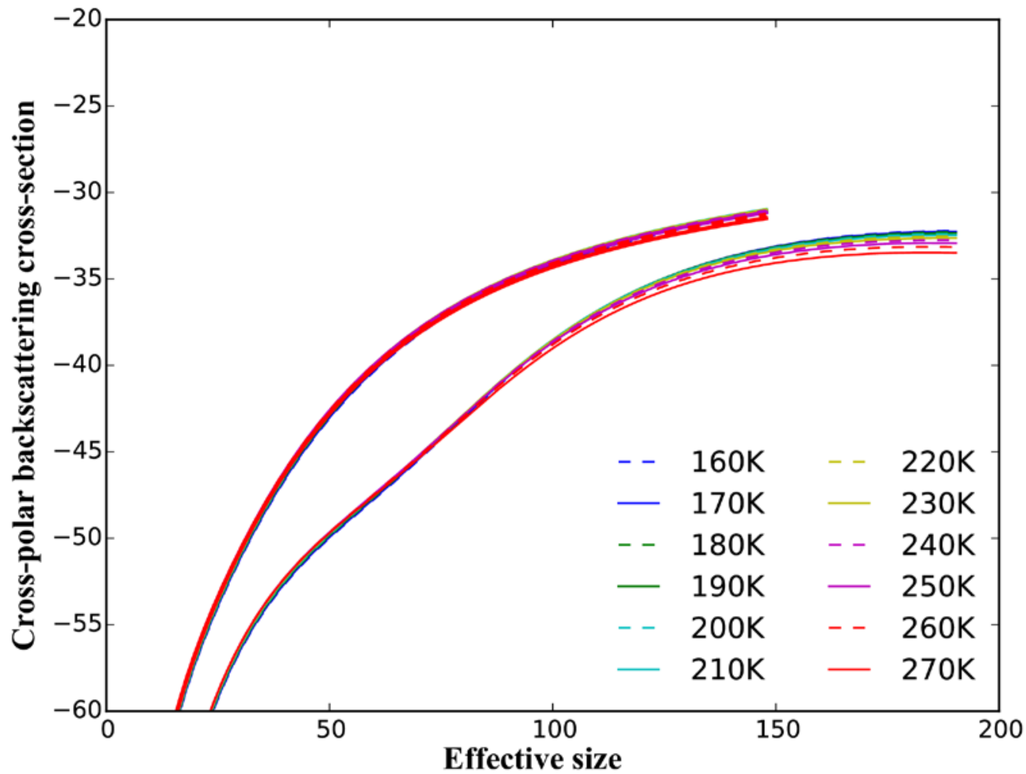

Figure 9. The same as Fig. 8 but showing the h-v polarization back scattering cross-section.

Conclusion and discussion

We provide in this paper a benchmark for future study about ice cloud retrievals using the 874GHz band. The sensitivities of optical properties of ice particles to temperature, particle shape, and size distribution are studied. Both scattering and absorption coefficients are shown to be sensitive to particle shape and size distribution. Moreover, the absorption coefficient is sensitive to temperature. This benefits the retrieval of ice water content from submillimeter radiometers. The co-polar back scattering cross-section is shown to be insensitive to either size distribution or particle shape in the range of 50-200μm in terms of D_{eff}, while the cross-polar back scattering cross-section is sensitive to both factors. This feature benefits retrieval of ice water content from meterological radars, which measure the co-polar back scattering cross-section.

Acknowledgements. This study was supported by NASA Grant NNX15AI54G.

References

[1] Myhre G, Shindell D, Bréon FM, Collins W, Fuglestvedt J, Huang J,., Zhang H. Anthropogenic and Natural Radiative Forcing. Climate change. 2013;423.

[2] Zhang Y, Macke A, Albers F. Effect of crystal size spectrum and crystal shape on stratiform cirrus radiative forcing. Atmospheric research. 1999;52(1):59-75.

[3] Wang C, Yang P, Platnick S, Heidinger AK, Baum BA, Greenwald T,., Holz RE. Retrieval of ice cloud properties from AIRS and MODIS observations based on a fast high-spectral-resolution radiative transfer model. Journal of Applied Meteorology and Climatology. 2013;52(3):710-726.

[4] Evans KF, Wang JR, Starr OC, Heymsfield G, Li L, Tian L,., Bansemer A. Ice hydrometeor profile retrieval algorithm for high-frequency microwave radiometers: application to the CoSSIR instrument during TC4. Atmospheric Measurement Techniques. 2012;5(9):2277-2306.

[5] Buehler SA, Jimenez C, Evans KF, Eriksson P, Rydberg B, Heymsfield AJ,., Davis CP. A concept for a satellite mission to measure cloud ice water path, ice particle size, and cloud altitude. Quarterly Journal of the Royal Meteorological Society. 2007;133(S2):109-128.

[6] Baum BA, Heymsfield AJ, Yang P, & Bedka ST. Bulk scattering properties for the remote sensing of ice clouds. Part I: Microphysical data and models. Journal of Applied Meteorology. 2005;44(12):1885-1895.

[7] Liu C, Yang P, Minnis P, Loeb N, Kato S, Heymsfield A, Schmitt C. A two-habit model for the microphysical and optical properties of ice clouds. Atmospheric Chemistry and

Physics. 2014;14(24):13719-13737.

[8] Baum BA, Kratz DP, Yang P, Ou SC, Hu Y, Soulen PF, Tsay SC. Remote sensing of cloud properties using MODIS airborne simulator imagery during SUCCESS: 1. Data and models. Journal of Geophysical Research: Atmospheres (1984--2012). 2000;105(D9):11767-11780.

[9] Liu G. A database of microwave single-scattering properties for nonspherical ice particles. Bulletin of the American Meteorological Society. 2008;89(10):1563-1570.

[10] Petty GW, Huang W. Microwave backscatter and extinction by soft ice spheres and complex snow aggregates. Journal of the Atmospheric Sciences. 2010;67(3):769-787.

[11] Kim M. Single scattering parameters of randomly oriented snow particles at microwave frequencies. Journal of Geophysical Research: Atmospheres (1984–2012). 2006;111(D14).

[12] Lu Y, Aydin K, Clothiaux EE, Verlinde J. Dielectric constant adjustments in computations of the scattering properties of solid ice crystals using the Generalized Multi-particle Mie method. ournal of Quantitative Spectroscopy and Radiative Transfer. 2014;135:1-8.

[13] Liu G. Approximation of single scattering properties of ice and snow particles for high microwave frequencies. Journal of the atmospheric sciences. 2004;61(20):2441-2456.

[14] Bi L, Yang P. Accurate simulation of the optical properties of atmospheric ice crystals with the invariant imbedding T-matrix method. Journal of Quantitative Spectroscopy and Radiative Transfer. 2014;138:17-35.

[15] Bi L, Yang P, Kattawar GW, Mishchenko MI. Efficient implementation of the invariant imbedding T-matrix method and the separation of variables method applied to large

nonspherical inhomogeneous particles. Journal of Quantitative Spectroscopy and Radiative Transfer. 2013;116:169-183.

[16] Mishchenko MI., Hovenier JW, and Travis LD, 2000: *Light scattering by nonspherical particles: theory, measurements, and applications*., Academic Press, 690pp.

[17] Baran AJ., 2009: A review of the light scattering properties of cirrus. Journal of Quantitative Spectroscopy and Radiative Transfer. 2009; 110:1239–1260.

[18] Ishimoto H, Masuda K, Mano Y, Orikasa N, and Uchiyama A, Irregular shaped ice aggregates in optical modeling of convectively generated ice clouds, Journal of Quantitative Spectroscopy and Radiative Transfer. 2012; 113:632-643.

[19] Zhang C, Lee KS, Zhang XC, Wei X, Shen YR. Optical constants of ice Ih crystal at terahertz frequencies. Applied Physics Letters. 2001;79(4):491-493.

[20] Iwabuchi H, Yang P. Temperature dependence of ice optical constants: Implications for simulating the single-scattering properties of cold ice clouds. Journal of Quantitative Spectroscopy and Radiative Transfer. 2011;112(15):2520-2525.

[21] Warren SG, Brandt RE. Optical constants of ice from the ultraviolet to the microwave: A revised compilation. Journal of Geophysical Research: Atmospheres (1984–2012). 2008;113(D14).

[22] Mätzler C. Thermal microwave radiation: applications for remote sensing. 2006.

[23] Rajaram B, Glandorf DL, Curtis DB, Tolbert MA, Toon OB, Ockman N. Temperature-dependent optical constants of water ice in the near infrared: new results and critical review of the available measurements. Applied Optics. 2001;40(25):4449-4462.

[24] Curtis DB, Rajaram B, Toon OB, Tolbert MA. Measurement of the temperature-dependent

optical constants of water ice in the 15–200 μm range. Applied Optics. 2005;44(19):4102-4118.

[25] Gosse S, Labrie D, Chylek P. Refractive index of ice in the 1.4–7.8-μm spectral range. Applied Optics. 1995;34(28):6582-6586.

[26] Clapp ML, Worsnop DR, Miller RE. Frequency-dependent optical constants of water ice obtained directly from aerosol extinction spectra. The Journal of Physical Chemistry. 1995;99(17):6317-6326.

[27] Toon OB, Tolbert MA, Koehler BG, Middlebrook AM, Jordan J. Infrared optical constants of H2O ice, amorphous nitric acid solutions, and nitric acid hydrates. Journal of Geophysical Research: Atmospheres (1984–2012). 1994;99(D12):25631-25654.

[28] Warren SG. Optical constants of ice from the ultraviolet to the microwave. Applied Optics. 1984;23(8):1206-1225.

[29] Stamnes K, Tsay SC, Wiscombe W, Jayaweera K. Numerically stable algorithm for discrete-ordinate-method radiative transfer in multiple scattering and emitting layered media. Applied Optics. 1988;27(12):2502-2509.